Broken vertex symmetry and finite zero-point entropy in the artificial square ice ground state

Sebastian Gliga, Attila Kákay, Laura J. Heyderman, Riccardo Hertel, and Olle G. Heinonen

Phys. Rev. B **92**, 060413 — Published 26 August 2015

DOI: 10.1103/PhysRevB.92.060413

Broken vertex symmetry and finite zero-point entropy in the artificial square ice ground state

Sebastian Gliga,[1,2,*] Attila Kákay,[3] Laura J. Heyderman,[1,2] Riccardo Hertel,[4] and Olle G. Heinonen[5,6]

[1] *Laboratory for Mesoscopic Systems, Department of Materials, ETH Zurich, 8093 Zurich, Switzerland*
[2] *Laboratory for Micro- and Nanotechnology, Paul Scherrer Institute, 5232 Villigen PSI, Switzerland*
[3] *Helmholtz-Zentrum Dresden-Rossendorf, Institute of Ion Beam Physics and Materials Research, Bautzner Landstraße 400, 01328 Dresden, Germany*
[4] *IPCMS UMR7504, CNRS and UdS, Strasbourg, France*
[5] *Materials Science Division, Argonne National Laboratory, Lemont, IL 60439, USA*
[6] *Department of Physics and Astronomy, Northwestern University, 2145 Sheridan Rd., Evanston, IL 60208-3112*

We study degeneracy and entropy in the ground state of artificial square spin ice. In theoretical models, individual nanomagnets are typically treated as single spins with only two degrees of freedom, leading to a two-fold degenerate ground state with intensive entropy and thus no zero-point entropy. Here, we show that the internal degrees of freedom of the nanostructures can result, through edge bending of the magnetization and breaking of local magnetic symmetry at the vertices, in a transition to a highly degenerate ground state with finite zero-point entropy, similar to that of the pyrochlore spin ices. We find that these additional degrees of freedom have observable consequences in the resonant spectrum of the lattice and predict the occurrence of edge 'melting' above a critical temperature at which the magnetic symmetry is restored.

PACS numbers: 75.78.Cd, 75.78.-n, 75.75.-c

Artificial spin ices are arrays of patterned nanoscale magnetic structures in which the geometrical arrangement leads to frustrated magnetic interactions[1,2]. One type of artificial spin ice is the *square ice*, consisting of magnetic nanoislands patterned on a square lattice[3–7] designed to mimic the frustration found in rare earth titanate pyrochlore systems. While the pyrochlore-based spin ices have been shown to have a finite zero-point entropy[8,9], this is not expected to be the case in artificial spin ices, due to their 'flat' geometry[10,11]. Here, we show that artificial square spin ice can equally exhibit a finite zero-point entropy in the ground state, and that this entropy can moreover be tailored through film thickness. It has recently been shown that entropy in pyrochlore compounds could be controlled in thin, single crystal epitaxial films in which the entropy can vanish at zero temperature owing to strain that removes the degeneracy[12]. In contrast to the pyrochlore spin ices, we attribute our findings to a change in the symmetry of the internal magnetic structure of the nanomagnets enabled by the existence of multiple degrees of freedom. Specifically, as the thickness of the nanoislands is increased, or the lattice constant of a square ice is reduced, the increased magnetostatic coupling leads to a transition from a symmetric magnetic state to a broken-symmetry state at each vertex. We find that this transition has a profound effect on the ground state, on the thermodynamics, and on the collective resonant modes of the square spin ice with experimentally accessible signatures.

Using micromagnetic modeling, we find that in artificial square ice arrays made of sufficiently thin nanostructures (or equivalently when the saturation magnetization, M_s, is small enough) the magnetization in each island is in a symmetric state (or 'onion' state[13]). This results in a twofold degenerate ground state in the square ice[14], as experimentally observed in ref.[7] and in a small intensive entropy, $S = k_B \ln(2)$, as expected from Ising models, such that the entropy per island vanishes in the thermodynamic limit. In contrast, in thicker structures (or for larger values of M_s), the magnetization in the nanoislands displays edge bending due to magnetostatic coupling between neighboring islands. This reduces the magnetic symmetry at each vertex and introduces a large, extensive degeneracy resulting in a finite zero-point entropy per island. Figure 1 shows the possible configurations of the magnetization in the nanoislands. The global structure of the ground state in square ice is illustrated in Fig. 1a. Focusing on the details of the magnetization at the edges of the islands at a vertex, Fig. 1b shows the computed symmetric state in islands only a few nanometers thick (labeled *e-0*) while Fig. 1c,d show the possible configurations when edge bending is present which we label *e-I* and *e-II*. This bending is due to the internal magnetic degrees of freedom in each island which are typically ignored in models of artificial spin ices where each nanomagnet is treated as a point or extended dipole. We find that these degrees of freedom have experimentally measurable effects, in particular in the spectrum of eigenmodes, from which the vertex configurations present in an array can be identified, thereby revealing the degeneracy of the system. Moreover, there is a temperature at which the bent edges 'melt', restoring the time-averaged magnetic symmetry. These results open new possibilities for tailoring collective behavior in artificial spin ice, for example for possible magnonic applications[15,16], and also sets limits on the applicability of models that do not take into account the internal degrees of freedom present in such systems.

We have investigated the dynamic behavior of the ground state of artificial square ice at $T = 0$ K

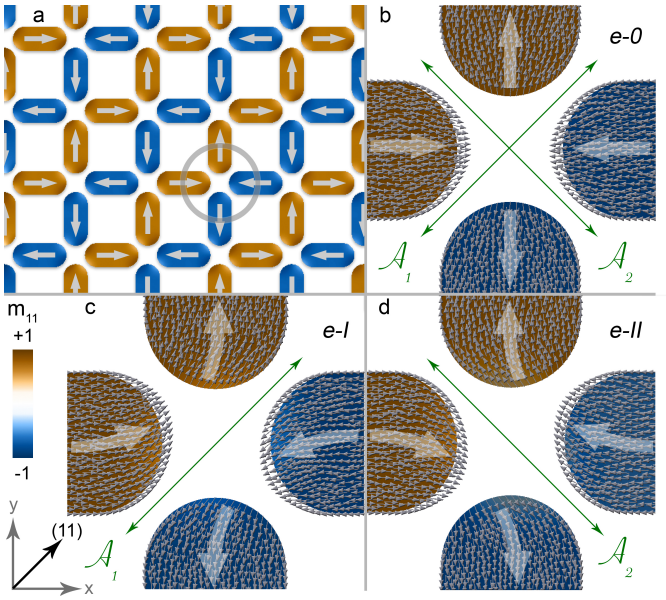

Figure 1. (a) Two-fold degenerate macroscopic ground state configuration in artificial square ice. The arrows represent the overall orientation of the magnetization within each island. The circle indicates the vertex enlarged in the subsequent images. (b) Microscopic structure of the magnetization at the edges of 4 nm-thick Permalloy nanoislands, in a symmetric state (labeled *e-0*). The small arrows represent the computed local magnetization, while the large arrows serve as a guide to the eye. Panels (c) and (d) show two possible degenerate configurations of the magnetization in strongly magnetostatically coupled islands (labeled *e-I* and *e-II*). While the magnetic configuration *e-0* has two magnetic symmetry axes, $\mathcal{A}_1$ and $\mathcal{A}_2$, *e-I* and *e-II* have a single axis, thus lowering the vertex symmetry.

using fully three-dimensional finite-element micromagnetic simulations based on the Landau-Lifshitz-Gilbert equation[15] considering an array of $N = 120$ stadium-shaped nanoislands (Fig. 1a) with dimensions 290 nm $\times$ 130 nm and variable thicknesses with a lattice constant of 276 nm. Each nanomagnet was discretized into tetrahedral elements, with an average cell size corresponding to an equivalent cube with 3 nm side length. The material parameters are typical for Permalloy: A=1.3 pJ/m, M_s=800 kA/m and zero magnetocrystalline anisotropy[17]. For the chosen lattice constant, islands thinner than approximately 14 nm are in a symmetric onion state, as shown in Fig. 1b. Considering that the magnetization is an axial vector, the vertex possesses two axes of magnetic symmetry $\mathcal{A}_1$ and $\mathcal{A}_2$. In thicker nanostructures (Fig. 1c,d), the increased magnetostatic coupling leads to a transition to magnetic states where the edge magnetization couples strongly to one of its nearest neighbors, breaking the local two-fold symmetry. Two energetically degenerate configurations, *e-I* or *e-II*, are possible which do not violate the ice rule[18] and possess a single symmetry axis. Edge bending[19] has been observed in Lorentz transmission electron microscopy imaging of artificial square ice lattice in a different context[20] and has been predicted to give rise to chiral vertex structures in kagome artificial spin ice[21]. The ground state entropy *per* vertex is therefore finite and equals $k_B \ln(2)$ in the thermodynamic limit, resulting in a finite zero-point entropy. This is in principle observable experimentally through calorimetry, but difficult to measure in practice because of the small sample volume and, hence, small heat capacity. We however find that the degeneracy, and thus the entropy, is easily and directly accessible through the spectrum of eigenmodes of the system. We have obtained resonant spectra by applying a short 5 mT field pulse along the (11) diagonal (see fig. 1) and subsequently integrating the Landau-Lifshitz-Gilbert equation for 15 ns. Starting with a square ice array in a ground state made only of *e-I* vertices, Fig. 2a shows the amplitude of the edge mode for this configuration while the computed spectrum in fig. 2b displays a peak at 3.1 GHz (grey filled spectrum). Then, *e-II*-type vertices are introduced one by one: this leads to a reduction in the intensity of the peak associated with the *e-I* vertices and an increase of the peak at 3.6 GHz, associated to the *e-II* vertices. Clearly the mode amplitudes and the change in the peak intensities are not symmetric owing to differences in the magnitude of the local field-induced torque, which results in a different variation of the local fields that drive the resonant dynamics. Indeed, for *e-I*, the edge magnetization of the islands is almost either parallel or antiparallel to the applied field direction (see Fig. 1c for the local direction of the magnetization), resulting in a small torque and a small excited area, while for *e-II*, the edge magnetization is almost perpendicular to the applied field (Fig. 1d), giving rise to a larger torque over a larger area. In Fig. 2c the evolution of the peak intensity associated with these two vertex types is plotted for two different field pulse directions: along the (11) and the (1-1) directions. For a field along (11), the evolution of the peak intensity is linear, with $\Delta I_{\mathrm{e-II}} > \Delta I_{\mathrm{e-I}}$. When the field angle is changed from the (11) to the (1-1) direction, the asymmetry in evolution is reversed. An arbitrary square spin ice system with broken-symmetry vertices will in general have a random distribution of vertex configurations. The existence of two peaks therefore serves as an unambiguous signature of the broken symmetry, while the relative intensities of these peaks can be used to determine the relative population of each vertex configuration. In contrast, the spectrum for a system with only symmetric *e-0* states is degenerate with respect to fields applied along the (11) and (1-1) directions and exhibits only a single peak around 2.6 GHz, as seen in Fig. 2d.

In addition to the dynamic signature in the mode spectrum, the internal degrees of freedom of the islands can also affect the thermal evolution of the system. Indeed, the two broken-symmetry configurations *e-I* and *e-II* are separated by an energy barrier whose magnitude is defined by the intermediate symmetric state. This energy barrier is set, for fixed M_s, by the thickness of the nanomagnets and the lattice constant. For a range of thick-

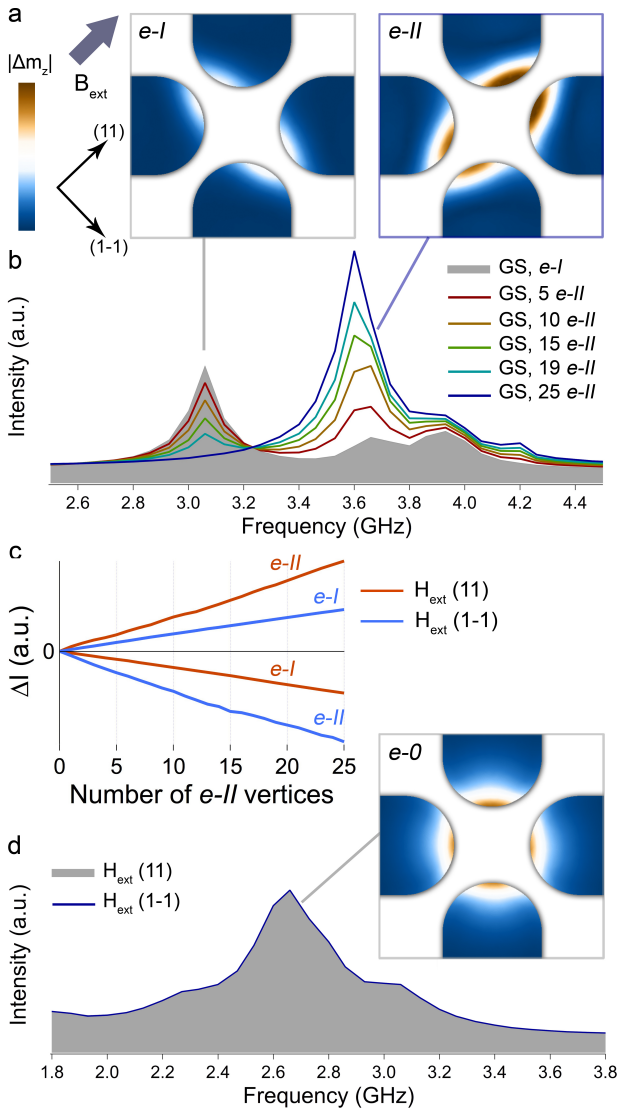

Figure 2. (a) Simulated (normalized) edge mode amplitudes for the *e-I* and *e-II* vertex configurations after applying an external field pulse along the (11) direction. (b) The ground state spectrum (grey) for a lattice only made of *e-I* type vertices displays a peak at 3 GHz. Introducing an increasing number of *e-II* vertices in the system leads to a decrease of the original mode intensity and to the evolution of a peak at 3.6 GHz corresponding to the mode associated to the *e-II* vertices. (c) Peak amplitude evolution of the two modes following pulses along the (11) (red curves) and (1-1) directions (blue curves) as a function of increasing number of introduced *e-II* vertices. (d) Ground state spectrum (grey) for a lattice with *e-0* type symmetric vertices following a pulse along (11). The spectrum is identical if the pulse is along (1-1) (blue). The insert shows the normalized edge mode amplitude.

nesses and lattice constants, this energy barrier can be tuned to be experimentally accessible. Figure 3 shows the micromagnetically computed energy barrier between the *e-I* and *e-II* states in a single vertex made of 470 nm × 170 nm islands. For example, for a thickness of 10 nm and a lattice constant of 425 nm, the energy barrier is calculated micromagnetically to be about 400 K. As the temperature is increased from below 400 K to above, the edges *melt*, *i.e.* the system can access both configurations *e-I* and *e-II* as shown in Fig. 4a,b. The time scale of the switching is defined by the temperature and is of approximately 10 ns at 400 K. One consequence of this is that, using observational techniques such as Lorentz transmission electron microscopy[20] or photoelectron emission microscopy[22], a time-averaged image on a time scale much larger than a few tens of ns will display a restored symmetry along the axis of each island, with the magnetization near the edges blurred out and averaged to zero. This

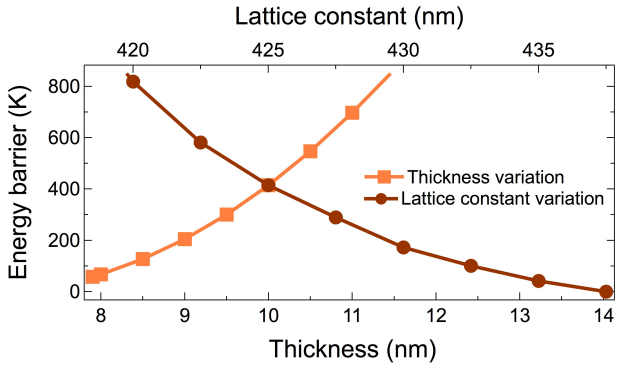

Figure 3. Energy barrier separating the *e-I* and *e-II* states as a function of island thickness and lattice constant in a square lattice with islands 470 nm × 170 nm. Islands with a thickness of 10 nm and a lattice constant of 425 nm (intersection of the two curves) and $M_s = 800$ kA/m were used in Fig. 4. Although the barrier is computed up to the Curie temperature, the validity of the used assumptions breaks down earlier, due to changes in the value of M_s.

change in symmetry of the system has a clear signature in the spectra of magnetization dynamics. As the temperature is increased from well below the energy barrier, magnetic fluctuations at the edge increase, and the magnetization eventually makes an excursion across the energy barrier. This leads to increased low-frequency noise in the magnetization spectrum (similar to Barkhausen noise), while the spectral peaks corresponding to resonant modes are not affected (other than a small thermal broadening).

Figure 4c shows spectra for a system in which the ground state has *e-I*-type vertices only. At 200 K, the spectrum shows a pronounced peak at about 1.5 GHz, corresponding to a resonance of the outer edges of the vertex islands. At 400 K, close to the melting temperature, the spectrum contains large low-frequency noise, corresponding to thermal fluctuations across the barrier, while the rest of the spectrum is almost identical to the low-temperature one at frequencies above ~ 1 GHz. The $1/f$-character of the low-frequency noise (Fig. 4d) indicates that the thermal activation is not of Arrhenius type; this $1/f$-type flicker noise likely arises from the coupled and incoherent dynamics of the magnetization degrees of

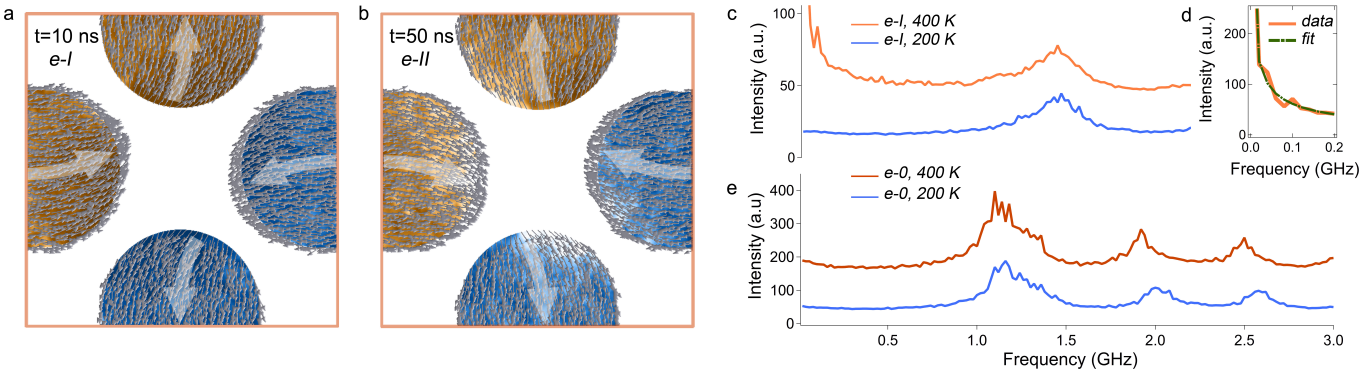

Figure 4. (a) Snapshot of the magnetic configuration of a square ice vertex made of 470 nm × 170 nm × 10 nm islands at 400 K. Thermal excitation was introduced at t=0 when the vertex was in the *e-I* state. (b) At t=50 ns, the vertex is in the *e-II* state. On longer time scales the time-averaged state restores the local symmetry indicating that the edges have melted. (c) Thermal magnetization dynamics spectra averaged over 1000 ns for a vertex with broken symmetry below (T=200 K) and at the edge melting temperature (T=400 K). The spectrum shows a dramatic increase in low-frequency noise as the temperature is increased, indicating thermal transitions across the energy barrier. (d) Low-frequency data below 0.2 GHz at 400 K and $1/f^{\alpha}$ fit with $\alpha \sim 0.7$. (e) Spectra for a vertex in a symmetric ground state (*e-0*). These display no significant temperature-dependent low-frequency noise.

freedom near the vertices, rather than coherent Stoner-Wohlfarth type behavior. Analysis of the dynamics at low frequencies suggests that the peak near 0.1 GHz in Fig. 4d corresponds to thermally-driven incoherent dynamics of the magnetization in the e-II configuration, in agreement with the average dwell time of the edges of approximately 10 ns. In contrast, the spectrum for a system for which the islands are in a symmetric state at $T = 0$ K does not exhibit such an increase in low-frequency noise as the temperature is increased, as seen in Fig. 4e at 200 K and 400 K. The peaks above ~ 1 GHz correspond to different edge mode contributions. Therefore, the appearance of low-frequency noise with increasing temperature is a clear observable experimental signature of edge melting.

While the described results are for ideal nanomagnet geometries, we expect them to hold in actual patterned systems that include structural disorder. Indeed, for small perturbations around the equilibrium, edge disorder won't have a decisive effect like for the magnetization reversal, where it can influence the reversal path[23] and we predict a slight broadening of the linewidth of the resonant peaks. In thermally active nanomagnets close to the edge melting temperature, roughness should lead to a broadening of the energy barriers which could slightly change the exponent, α, of the low-frequency noise as expected from a distribution of energy barriers.

In conclusion, using detailed micromagnetic modeling, we have demonstrated that an artificial square spin ice lattice can undergo a transition from a two-fold degenerate ground state to a broken-symmetry, highly degenerate ground state with finite zero-point entropy per island. This transition is driven by magnetostatic interactions between nearest-neighbors at vertices and can be induced by increasing the film thickness, decreasing the lattice constant, or increasing the saturation magnetization. It arises from the internal degrees of freedom of the magnetic nanostructures which are typically absent in models that consider the magnetization to be uniform. We find that the symmetry at each vertex gives rise to clear signatures in the resonant dynamics spectrum, providing a means to distinguish between the presence and absence of symmetry and to determine the number of vertices with a specific magnetic configuration. Moreover, we predict the existence of edge melting above a certain temperature at which the time-averaged symmetry of the system is restored. The experimental signature of this edge melting should be an increased low-frequency noise with increasing temperature. We anticipate that the existence of internal magnetic degrees of freedom might equally lead to unexpected static and dynamic properties in other frustrated systems, such as for example in kagome ice as well as in modified artificial spin ice geometries[24].

S. G. wishes to thank Armin Kleibert for fruitful discussions about the experimental implications of this work. The work by O. H. was funded by the Division of Materials Science and Engineering, Department of Energy Basic Energy Sciences. We gratefully acknowledge the computing resources provided on Blues and Fusion, high-performance computing clusters operated by the Laboratory Computing Resource Center at Argonne National Laboratory.

* sebastian.gliga@psi.ch

[1] C. Nisoli, R. Moessner, and P. Schiffer, Rev. Mod. Phys.

85, 1473 (2013).
[2] L. J. Heyderman and R. L. Stamps, Journal of Physics: Condensed Matter **25**, 363201 (2013).
[3] R. F. Wang, C. Nisoli, R. S. Freitas, J. Li, W. McConville, C. B. J., M. S. Lund, N. Samarth, C. Leighton, V. H. Crespi, and P. Schiffer, Nature **439**, 303 (2006).
[4] G. Möller and R. Moessner, Phys. Rev. Lett. **96**, 237202 (2006).
[5] A. Remhof, A. Schumann, A. Westphalen, H. Zabel, N. Mikuszeit, E. Y. Vedmedenko, T. Last, and U. Kunze, Phys. Rev. B **77**, 134409 (2008).
[6] J. P. Morgan, A. Stein, S. Langridge, and C. H. Marrows, Nature Physics **7**, 75 (2011).
[7] A. Farhan, P. M. Derlet, A. Kleibert, A. Balan, R. V. Chopdekar, M. Wyss, J. Perron, A. Scholl, F. Nolting, and L. J. Heyderman, Phys. Rev. Lett. **111**, 057204 (2013).
[8] A. P. Ramirez, A. Hayashi, R. J. Cava, R. Siddharthan, and B. S. Shastry, Nature **399**, 333 (1999).
[9] G. C. Lau, R. S. Freitas, B. G. Ueland, B. D. Muegge, E. L. Duncan, P. Schiffer, and R. J. Cava, Nature Physics **2**, 249 (2006).
[10] G.-W. Chern, C. Reichhardt, and C. Nisoli, Appl. Phys. Lett. **104**, 013101 (2014).
[11] D. Thonig, S. Reißaus, I. Mertig, and J. Henk, Journal of Physics: Condensed Matter **26**, 266006 (2014).
[12] L. Bovo, X. Moya, D. Prabhakaran, Y. A.Soh, A. T. Boothroyd, N. D. Mathur, G. Aeppli, and S. T. Bramwell, Nat Commun. **5**, 3439 (2014).
[13] J. K. Ha, R. Hertel, and J. Kirschner, Phys. Rev. B **67**, 224432 (2003).
[14] L. A. Mól, R. L. Silva, R. C. Silva, A. R. Pereira, W. A. Moura-Melo, and B. V. Costa, Journal of Applied Physics **106**, 063913 (2009).
[15] S. Gliga, A. Kákay, R. Hertel, and O. G. Heinonen, Phys. Rev. Lett. **110**, 117205 (2013).
[16] M. Krawczyk and D. Grundler, J. Phys.: Condens. Matter **26**, 123202 (2014).
[17] Similar results were also obtained using a fast Fourier transform method on a cubic lattice, with a mesh size of 1.25 nm, in order to account for the magnetostatic effects near the curved boundaries of the nanoelements with high accuracy. [R. E. Camley, B.V. McGrath, Y. Khivintsev, Z. Celinski, R. Adam, C. M. Schneider, and M. Grimsditch, Phys. Rev. B **78**, 024425 (2008)].
[18] The different configurations are degenerate in energy if the edges of an individual island are exchange-decoupled, *i.e.* when the length of the nanoisland is much larger than the exchange length of the material.
[19] S. Hankemeier, R. Frömter, N. Mikuszeit, D. Stickler, H. Stillrich, S. Pütter, E. Y. Vedmedenko, and H. P. Oepen, Phys. Rev. Lett. **103**, 147204 (2009).
[20] C. Phatak, A. K. Petford-Long, O. Heinonen, M. Tanase, and M. De Graef, Phys. Rev. B **83**, 174431 (2011).
[21] N. Rougemaille, F. Montaigne, B. Canals, M. Hehn, H. Riahi, D. Lacour, and J.-C. Toussaint, New J. Phys. **15**, 035026 (2013).
[22] A. Farhan, P. M. Derlet, A. Kleibert, A. Balan, R. V. Chopdekar, M. Wyss, L. Anghinolfi, F. Nolting, and L. J. Heyderman, Nature Physics **9**, 1 (2013).
[23] K. K. Kohli, A. L. Balk, J. Li, S. Zhang, I. Gilbert, P. E. Lammert, V. H. Crespi, P. Schiffer, and N. Samarth, Phys. Rev. B **84**, 180412 (2011).
[24] M. J. Morrison, T. R. Nelson, and C. Nisoli, New Journal of Physics **15**, 045009 (2013).